Hydrol. Earth Syst. Sci. Discuss., 12, 5629–5670, 2015
www.hydrol-earth-syst-sci-discuss.net/12/5629/2015/
doi:10.5194/hessd-12-5629-2015

Hydrology and Earth System Sciences
Open Access
Discussions

Assessing the quality of Digital Elevation Models obtained from mini-Unmanned Aerial Vehicles for overland flow modelling in urban areas

J. P. Leitão, M. Moy de Vitry, A. Scheidegger, and J. Rieckermann

Eawag: Swiss Federal Institute of Aquatic Science and Technology, Überlandstrasse 133, 8600 Dübendorf, Switzerland

Received: 30 April 2015 – Accepted: 17 May 2015 – Published: 12 June 2015

Correspondence to: J. P. Leitão (joaopaulo.leitao@eawag.ch)

Published by Copernicus Publications on behalf of the European Geosciences Union.

Abstract

Precise and detailed Digital Elevation Models (DEMs) are essential to accurately predict overland flow in urban areas. Unfortunately, traditional sources of DEM remain a bottleneck for detailed and reliable overland flow models, because the resulting DEMs are too coarse to provide DEMs of sufficient detail to inform urban overland flows. Interestingly, technological developments of Unmanned Aerial Vehicles (UAVs) suggest that they have matured enough to be a competitive alternative to satellites or airplanes. However, this has not been tested so far. In this this study we therefore evaluated whether DEMs generated from UAV imagery are suitable for urban drainage overland flow modelling. Specifically, fourteen UAV flights were conducted to assess the influence of four different flight parameters on the quality of generated DEMs: (i) flight altitude, (ii) image overlapping, (iii) camera pitch and (iv) weather conditions. In addition, we compared the best quality UAV DEM to a conventional Light Detection and Ranging (LiDAR)-based DEM. To evaluate both the quality of the UAV DEMs and the comparison to LiDAR-based DEMs, we performed regression analysis on several qualitative and quantitative metrics, such as elevation accuracy, quality of object representation (e.g., buildings, walls and trees) in the DEM, which were specifically tailored to assess overland flow modelling performance, using the flight parameters as explanatory variables. Our results suggested that, first, as expected, flight altitude influenced the DEM quality most, where *lower flights* produce better DEMs; in a similar fashion, *overcast* weather conditions are preferable, but weather conditions and other factors influence DEM quality much less. Second, we found that for urban overland flow modelling, the UAV DEMs performed competitively in comparison to a traditional LiDAR-based DEM. An important advantage of using UAVs to generate DEMs in urban areas is their flexibility that enables more frequent, local and affordable elevation data updates, allowing, for example, to capture different tree foliage conditions.

HESSD
12, 5629–5670, 2015

1 Introduction

1.1 Urban drainage modelling

Densely urbanised areas, where most economic activities take place, face high probability of flood occurrence due to: (i) the large percentage of impervious areas, which consequently increase the runoff volume; and (ii) alterations of natural water streams and existence of sewer systems which increase flow velocities, thus reducing catchments' time of concentration and duration of the critical rainfall events. In addition, climate change may increase rainfall intensity and frequency in some regions of the Globe, which will affect ecosystems and human life. These more frequent extreme conditions can ultimately increase the probability that urban drainage system capacity is exceeded, which may lead to higher urban flood risks (when flood consequences are maintained).

Hydrological and hydraulic models are important tools to estimate urban flood risk and help engineers and decision makers designing urban drainage systems that inherently reduce these risks. Urban drainage models should be represented by coupling the sewer system (one-dimensional model, 1-D) with the overland flow system (1-D or two-dimensional models, 2-D). Several studies have tested and compared different urban drainage modelling approaches (e.g. Apel et al., 2009; Hunter et al., 2008; Allitt et al., 2009), such as 1-D sewer system (e.g., Vojinović and Tutulić, 2009), coupled 1-D sewer system with 1-D overland flow system (1-D/1-D) (e.g., Maksimović et al., 2009; Leandro et al., 2009) and coupled 1-D sewer system with 2-D overland flow system (1-D/2-D) (e.g., Chen et al., 2007). The different coupled modelling approaches rely on the quality of the Digital Elevation Model (DEM) to represent the terrain and then locate flood-prone areas – this is especially important for local (and more frequent) floods when compared to large floods (e.g., fluvial, coastal flooding, or a combination of these two types).

HESSD
12, 5629–5670, 2015

1.2 Model input elevation data sources and UAVs

From the literature, it is clear that a great effort has been made to develop new and improve existing numerical solutions for hydraulic models. However, DEMs, as all input data, may have a significant impact on overland flow modelling results (Fewtrell et al., 2011; Leitão et al., 2009). Leitão et al. (2009) showed the effect that DEM sources, resolution and accuracy have on the delineation of overland flow paths in urban catchments; fine resolution DEMs are required to obtain accurate 1-D overland flow networks in urban areas. Fewtrell et al. (2011) who evaluated two different hydraulic models on a DEM of resolution varying from 0.5 to 5 m, also concluded that the data resolution has a greater effect on results than the model used, especially if not calibrated. While it is evident that the representation of roads is critical, requiring a minimum resolution of 2 to 3 m, walls and street curbs are also elements that influence the propagation of a flood wave (Sampson et al., 2012), but to represent these elements in the DEM, a finer resolution (< 1 m) is required. Realistic and detailed representation of terrain plays thus a fundamental role in overland flow modelling.

Interestingly, DEMs with a resolution finer than 1 m suitable for urban overland flow modelling can now be generated using imagery captured with Unmanned Aerial Vehicles (UAVs). UAVs are uninhabited aircrafts that are reusable; thereof their operation can be either autonomous, remote controlled, or a combination of the two.

The recent developments of UAVs and their increasing availability make them a new potential source of terrain elevation data. The fine spatial resolution than can be obtained (e.g., 0.05 m) is well-suited to conduct detailed urban overland flow studies. Furthermore, UAVs make repeated flights feasible to capture different conditions, such as tree leaves-off or tree-leaves-on conditions, and better characterize impervious areas, which is important for urban flood modelling, and they can be applied in remote areas. The handling of UAVs is simplified to a degree that can be managed by non-expert professionals, such as civil engineers and engineering consultants.

HESSD
12, 5629–5670, 2015

1.3 Generation of very fine-resolution digital elevation models using UAV imagery

1.3.1 Photogrammetric process

Photogrammetry is often the preferred methodology when collecting three-dimensional (3-D) data using UAVs. Photogrammetry produces 3-D point clouds based on overlapping images. Other useful by-products can be derived, such as urban façade textures (Leberl et al., 2010). For UAV's, photogrammetry is an interesting alternative to the predominant LiDAR (Light Detection and Ranging) method. LiDAR techniques are precise and allow for multi-returns – e.g., in areas with trees the ground elevation can be automatically measured. However, due to the weight and high-energy demand of LiDAR devices, there are not adequate for UAVs and impossible to use with mini-UAVs. On the other hand, the images can be taken with light equipment (e.g. consumer cameras) that does not require high energy. The question of photogrammetry vs. LiDAR has been raised and discussed in a few past publications (Baltsavias, 1999; Leberl et al., 2010; Küng et al., 2011). Specific applications of UAV photogrammetry are presented in Remondino et al. (2011).

The main photogrammetry steps to generate 3-D elevation models from overlapping images are presented in Küng et al. (2011):

1. Images are scanned for characteristic points, such as, for example, marks created in the ground specifically to support the survey or manholes. If Ground Control Points (GCPs) are used to geo-reference the model, they are usually labelled in the images before this step.

2. Based on the characteristic points, image geo-information and the known camera parameters, a sparse point cloud model is derived with a so-called bundle block adjustment algorithm (Triggs et al., 2000). It is sparse since formed only of the characteristic points from step 1.

HESSD
12, 5629–5670, 2015

3. Based on the sparse point cloud, dense image matching is performed to increase the spatial resolution of the point cloud model and the 3-D elevation model generated.

1.3.2 Digital elevation model generation process

The resulting point cloud may contain errors, such as image shadows, mismatches and lens distortion. Therefore, algorithms for outlier removal and smoothing can be applied. If a Digital Surface Model (DSM) is required, vegetation, buildings, and other objects need to be filtered out. Finally, the resulting point cloud is triangulated to a triangulated irregular network (TIN), which may then be rasterised and used, for example, in hydraulic modelling software.

1.4 Study objectives

In this paper we aim at demonstrating the benefit of using high-resolution DEMs produced from mini-UAV acquired data on urban drainage modelling, as opposed to DEMs based on standard aerial LiDAR elevation data. Specifically, our study presents three distinct novelties.

- First, to the best of our knowledge, it uses for the first time DEMs produced from UAV photogrammetry in the context of urban drainage – more specifically on overland flow modelling.
- Second, it presents dedicated field experiments specifically tailored to understand how UAV flight parameters affect DEM quality and, eventually, overland flow representation.
- Third, it compares the quality of the UAV obtained DEM with a DEM used by Swiss engineers (LiDAR-based DEM) and discusses advantages and disadvantages for urban drainage and flood modelling.

HESSD
12, 5629–5670, 2015

Our results suggested that UAVs are a very promising technology for our purpose and that results are relatively robust to not optimal flight parameters. Given the current developments, we expect that the quality of the products generated using these systems will quickly improve in the near future due to better software that manufacturers provide together with the UAV platforms. However, important limitations might arise from regulatory affairs. This will also be discussed below.

This paper is organised as follows: Sect. 2 describes the methods proposed in this study to evaluate the UAV DEM and assess the impact of flight parameters on DEM quality. In Sect. 3 the case study location and the flight parameters are presented; UAV and camera used are also described in this section. Analysis of findings are presented and discussed in Sect. 4. Finally, Sect. 5 summarises the major findings of the study, identifying also potential further research.

2 Methods

2.1 Impact of UAV flight parameters on DEM generation for overland flow modelling

The adequacy of a DEM for urban urban flood assessment cannot be defined objectively as the existing criteria (e.g., elevation, slope or aspect differences to a benchmark DEM) are not specific to each of the possible DEM applications. As a pragmatic solution, we propose a set of four qualitative and four quantitative evaluation metrics to evaluate the DEM quality. First, DEM values were compared with field measurements using, for example mean absolute errors and visual classification. Second, two statistical models were developed to explore the relations between the flight parameters and the DEM quality through the evaluation metrics: (i) an odds logistic regression model was applied for the qualitative metrics and (ii) a linear regression model was used to evaluate the quantitative metrics.

HESSD
12, 5629–5670, 2015

2.1.1 Qualitative metrics to assess DEM for overland flow modelling

Representation of voids between two closely located objects. This metric describes the space between two closely placed objects, such as buildings. This is an essential feature of a good-quality DEM for overland flow modelling, as in many flood events water flows through such small openings, which, consequently, can have a significant impact on the modelling results.

Quality of building edges representation. Building edges can be subject to distortions and to a "salt and pepper" effect caused by multiple 3-D points being identified one over the other; this is commonly associated with pixel-based classifications (de Jong et al., 2001). This metric describes the severity of building wall distortion and is important to assess the quality of the representation of linear features in the DEM which can divert overland flow.

Representation of walls. Walls are very relevant for overland flow modelling because they can obstruct and redirect water movement. This metric describes to what extent these elements are represented in the DEM.

Presence of trees. This metric describes whether trees are represented in the DEM, or not. It is desirable not to have trees represented because tree canopies, which are what is represented in the DEMs, do not influence overland flow.

The qualitative metrics were calculated based on a visual analysis of the DEM; a class was assigned to each analysis location. The classes are on an ordinal scale, where class 0 is the least favourable and class 3 the best class (Table 1).

2.1.2 Quantitative metrics to assess DEM for overland flow modelling

The following quantitative metrics may be considered a first attempt to define objective evaluation criteria to assess DEM quality for overland flow modelling. The metrics aim at describing the deviations from the reality of the representation of terrain features that may influence overland flow.

HESSD
12, 5629–5670, 2015

Absolute elevation differences. The vertical correctness of the DEM is relevant for urban drainage modelling. Suitable reference elevation data can be surveying points and a sewer manhole cadastre. In our case study, the vertical precision of the surveying points was given for each point and varied between 0.5 and 3 cm (1σ). The vertical accuracy of the manholes is not known; however, it is assumed to have a standard deviation of 7.5 cm (VBS, 2008).

Curb height differences. The height difference between road and sidewalk is relevant for relatively low overland flow, as in urban areas roads act as channels; only for large overland flow events (e.g. flooding events) the runoff will flow over sidewalks. Curb heights can be measured repeatedly at various locations in the area of study. To assess the curb height from the different DEMs representing different flight parameters, the average elevation difference between 1 m^2 areas on the road and on the sidewalk close to the curb height measurement location was calculated.

Flow direction (i.e. terrain aspect). Flow direction was measured on the field by pouring water and measuring orientation of flow direction with a compass (see Fig. 1a). In the DEM, the aspect was calculated, based on a 3×3 cell moving window (Burrough and McDonnell, 1998).

Flow path delineation. It is important that delineated flow paths are properly represented (mainly along the side of the roads), so that modelled overland flow runs into (or pass by in the vicinity of) sewer inlets. To assess the representativeness of the DEM-based delineated flow paths, real flow paths were observed by pouring water onto the road (Fig. 1a) and measuring the distance between the stabilized flow and the road curb (j in Fig. 1b). Often, the water flowed exactly on the side of the road. In the DEM, water flow paths were estimated using the flow accumulation method (Jenson and Domingue, 1988).

HESSD
12, 5629–5670, 2015

2.1.3 Statistical models

To identify the important flight parameters that determine DEM quality, two simple statistical models were used; one for the qualitative and a different one for the quantitative assessments.

Because the qualitative metrics are measured on an ordinal scale, the influence of the flight parameters was investigated with a proportional odds logistic regression model (see, e.g., Venables and Ripley, 2002). This model considers the natural order of the metrics, e.g. that class 3 is better than class 2. The probability that the jth observation of metric Y is at least as good as class k is modelled as

$$P(Y_j \leq k) = \frac{1}{1 + \exp\left(\varsigma_k - \eta_j\right)} \tag{1}$$

where the thresholds $\varsigma_0 = -\infty < \varsigma_1 < \cdots < \varsigma_4 = \infty$ are coefficients that are estimated additionally to the *coefficients* of the linear predictor η_j which is defined in Eq. (2).

For every quantitative metric, a linear regression model was setup to model the absolute differences between the values obtained from the DEM and the corresponding ones measured in the field

$$\eta_j = \beta_0 + \beta_1 z_{j1} + \beta_2 z_{j2} + \cdots + \beta_r z_{jr} \tag{2}$$

$$Y_j = \eta_j + \epsilon_j \tag{3}$$

where z_{jr} are the corresponding explanatory variables for the jth observation, ε is a Gaussian random error term and the β_r, $r = 0, 1, \ldots, r$ regression coefficients to be estimated. As explanatory variables all five flight parameters (i) flight altitude, (ii) camera pitch, (iii) frontal and (iv) lateral overlap, and (v) weather conditions (see Sect. 3.3) were used. As the *weather condition* provides qualitative information, it was included using dummy variables (see, e.g., Montgomery et al., 2012).

HESSD
12, 5629–5670, 2015

2.2 Comparison between a UAV DEM and a conventional LiDAR-based DEM

The DEMs used for the comparison have distinct characteristics. The smallest UAV DEM pixel size was 5 cm, whereas the LiDAR DEM[1] had a pixel size of 2 m.

The UAV DEM was generated based on flight 4 data (see Table 3), after a thorough comparison of the different flights (Moy de Vitry, 2014), which showed the good quality of the DEM produced from this flight. The UAV flight 4 was performed with the following settings:

- Flight altitude: 145 m (corresponds to a ground sampling distance of approximately 5 cm);
- Camera pitch: 15°;
- Image overlapping: 70 and 80 % frontal and lateral overlapping, respectively;
- Weather conditions: clear.

The LiDAR DEM is a 3-D height model that covers the whole Switzerland at a resolution of one data point per 2 m^2 and was then interpolated from the raw model to generate a 2 m raster grid. It is provided by Swisstopo[2] and represents all stable and visible landscape elements such as soil, natural cover, woods and all sorts of built infrastructure, such as buildings. The data acquisition method used is aerial LiDAR with a vertical accuracy of ± 0.5 m (1σ) in open terrain, and in terrain with vegetation the vertical accuracy is ± 1.5 m (1σ).

To compare the two DEMs, we built on the work of Podobnikar (2009), who discuss various visual assessment methods for identifying problems in DEMs that are otherwise not measured, like discontinuities. Also we used suggestions by Reinartz

[1] Swiss Federal Office of Topography (Article 30, Geoinformation Ordinance).

[2] http://www.swisstopo.admin.ch/internet/swisstopo/en/home/products/height/dom_dtm-av.html

HESSD
12, 5629–5670, 2015

et al. (2010) who used elevation differences and several terrain properties, like slope and land cover to compare two DEMs. Specifically, we used the following metrics for this specific purpose:

a. Visual DEMs comparison with hillshade[3];

b. Elevation differences between the two DEMs for diverse land uses (absolute differences and mean absolute differences);

c. Slope and aspect differences between the two DEMs. These two terrain surface characteristics are essential when considering overland flow modelling as they are associated with flow speed and direction, respectively, and

d. Delineation of flow paths. The flow paths were delineated using the D8 flow direction algorithm (Jenson and Domingue, 1988). This metric is meant to help understanding the correctness of overland flow representation.

To compute the values for metrics (*b*) and (*c*), the 2 m downsampled UAV DEM was used to match the resolution of the LiDAR DEM used in the comparison.

3 Material: UAV and case study

3.1 Unmanned aerial system

3.1.1 General

The mini-UAV platform, called "eBee", (from year 2013) developed by senseFly was used in this study. The eBee UAV is a fully autonomous fixed-wing electric-powered aircraft, with a wingspan of 0.96 m and weighs approximately 0.7 kg including a payload of 0.15 kg. The UAV can cover relatively large areas in a reasonable amount of time

[3]A hillshade is a greyscale visualization of the 3-D surface, with a lateral light source.

HESSD
12, 5629–5670, 2015

(maximum of 12 km^2 per 50 min flight – this value is strongly related to flight altitude and, consequently, to maximum image resolution), which is important for the economic viability of UAV remote sensing. Detailed information about the UAV used in this study is presented in Appendix A.

We selected this specific Unmanned Aerial System over other platforms for two main reasons. First, it is delivered as a complete system with flight planning and photogrammetry software, designed to work seamlessly with one another in a straightforward and intuitive way and does not requiring flying expertise. Second, the construction of the UAV itself provides passive safety, because it is lightweight and electric powered, has a foam body and, most important, glides if out of power. In addition, the autopilot has built-in safety procedures; which is crucial for flights over urban areas.

3.1.2 Camera

The UAV was equipped with a customised Canon IXUS 127 HS that is triggered by the UAV autopilot. The camera has RGB bands and operates in auto mode, making, for example, the photo exposure (e.g., speed and aperture) different from photo to photo. Thus it is not possible to configure the settings for a given flight; for that, a different camera would be required. Detailed characteristics of the camera are presented in Appendix A.

3.1.3 Photogrammetry software

The photogrammetry tasks, such as bundle block adjustment, point cloud generation and filtering were performed using the *Pix4-D*[4] *software* ((Küng et al., 2011)). This is one of the leading software for UAV photogrammetry (Sona et al., 2014); its main strength is a good handling of rather imprecisely referenced images.

[4] http://pix4d.com/

HESSD
12, 5629–5670, 2015

3.2 The case study area

Adliswil is a city near Zurich (Switzerland) and was chosen to be the case study area mainly because (i) it is a typical, rapid growing Swiss city (approx. 20 000 inhabitants) that (ii) needed up-to-date elevation data to be used in other urban drainage studies. Six areas in Adliswil were initially considered and evaluated to conduct the UAV flights. The experimental area was selected based on several criteria related to overland flow, such as including different road types and sidewalks, different terrain types, significant terrain elevation difference, high road density and roads that are relatively free of cars. In addition, practical criteria, such space for UAV taking-off and landing, visibility of UAV during flight from the take-off point had to be considered. The chosen location has an area 0.04 km^2 (approx. 130 × 300 m) and is illustrated in Fig. 2.

The case study location is outside the Swiss Air controlled zone[5], hence no permission was required to fly the UAV, as long as it always remained in line-of-sight.

3.3 Experimental field work: flights with different parameters

In total, 14 flights were conducted (flights 1 to 14) on the case study area to test the influence of flight parameters on the adequacy of DEMs for overland flow modelling. The flight parameters considered in this study are presented as follows.

Flight altitude. The flight altitude is one of the main factors that determines the scale and accuracy of the point cloud (Kraus, 2004); it is directly related to the Ground Sampling Distance (GSD). Therefore it is expected that a low flight altitude will have a positive influence on the representation of the terrain details on DEMs. In theory, flight heights of up to 1000 m are possible with the eBee. There is no lower limit, although safety and image overlap (the camera frequency is limited) become issues below 70 m above ground. In Switzerland, line-of-sight flight is required by the legislation, which limits the maximum elevation that is typically reached in flight.

[5]http://www.skyguide.ch

HESSD
12, 5629–5670, 2015

Camera pitch. Camera pitch can be assumed to have influence on the representation of steep surfaces; high values of camera pitch are assumed to generate better representations of steep surfaces, such as façades. While façades are of limited interest in urban drainage modelling, it is of interest to see whether camera pitch variation affects the representation of objects, such as cars or walls, which influence overland flow. With the eBee, the camera pitch can be defined between 0 and 15°.

Frontal image overlapping. Image overlapping determines the number of times a point on the ground can be captured on an image. It is therefore an important parameter influencing the accuracy of 3-D reconstruction. Frontal overlap is that in the direction of flight. In order to achieve acceptable matching between images, it is recommended to have a frontal overlap of 60 % or more. This lower limit should be increased in the case of complex terrain (for example forest).

Weather conditions. Lighting and the presence of shadows may have a strong effect on photogrammetry results. We deliberately did not adjust the flight plans to weather conditions. All the flights took place within a two days' time interval; some of the flights were performed under cloudy conditions whereas others were performed with direct sunlight.

Additionally to the 14 flights, two virtual flights (flight 15 and flight 16) were generated from two of the 14 flights to simulate the effect of image overlapping. Flight 15 was generated from every third flight line of flight 14. Similarly, flight 16 was generated from every third image from flight 11. The parameters of all 16 flights are presented in Table 2.

4 Results and discussion

In this section we first present the results of the influence of parameters on DEM quality, and second the results from the comparison of the UAV DEM to the LiDAR DEM.

HESSD
12, 5629–5670, 2015

4.1 Impact of UAV flight parameters on DEM generation for overland flow modelling

The statistical models set up for the qualitative metrics showed that, as expected, lower flight altitude produces better DEMs for overland flow modelling; lower flights tend to increase the quality of the DEM (Fig. 3a).

Also, flights performed under overcast conditions led to better results (Fig. 3b), most likely due to the more uniform illumination and absence of hard shadows.

Surprisingly, none of the quantitative metrics could have been related to the flight parameters. This may indicate that the variability of the metrics between flights with the same parameters is larger than the influence of the parameters; one can also say that the performance of the UAV is robust regarding the flight configuration.

The camera mounted in the UAV is a *point&shoot* consumer camera; we expect that we would have observed larger differences if a better camera had been used. For example, a better camera could have been operated with manual exposure, settings, and would have produced more equally exposed images. This alone could have substantially improved the identification of characteristic points.

4.2 Comparison between UAV DEM and LiDAR DEM

The objective of comparing the UAV DEMs and a nation-wide available and commonly used DEM is to evaluate whether UAV DEMs have a similar or better quality, especially in the urban areas which are relevant for overland flow modelling.

We expect that DEMs made available nation-wide (e.g., data sets provided by Swisstopo: the Swiss Federal Office of Topography[6]) are always less accurate in the vertical dimension ($0.5 < \sigma < 1.5$ m) than the DEMs generated based on UAV imagery. Experience shows that the vertical accuracy of the latter is usually about two to three times

[6] www.swisstopo.ch

HESSD
12, 5629–5670, 2015

the GSD (Pix4-D Support Team, 2014), which corresponds to a standard deviation of 0.1 to 0.2 m for the DEMs of our case study.

4.2.1 Visual comparison

It is possible to qualitatively assess the quality of a DEM using *hillshaded* DEMs (Fig. 4). One clear difference between the two DEMs is that the terrain along a water stream (① in Fig. 4) is not well represented in the UAV DEM. Another clear difference is that existing trees are represented in the LiDAR DEM and no trees seem to be represented in the UAV DEM in this area. This may be explained by the following considerations:

1. The trees growing on both sides along the water stream may have hindered a clear view of the terrain surface, thus contributing to the irregular representation of terrain, mainly due to the lack of common points used in the image matching (i.e., orthorectification) process.

2. The shadows captured in the images used in the orthorectification on the left side of the water stream might also have contributed to this problem. In order to confirm this, other flights, and corresponding DEMs, would need to be evaluated.

The tree-leaves-off conditions during the UAV flight in early March makes it difficult to identify matching points in the canopy/on bare thin branches which are often less wide than the GSD. Not having the tree canopies represented is though not a problem for overland flow modelling.

4.2.2 Elevation comparison

The map of the elevation differences between the UAV DEM and the LiDAR DEM (Fig. 5) was calculated subtracting the LiDAR DEM from the UAV DEM (Eq. 4) with 2 m pixel^{-1} resolution (Fig. 4b).

$$\Delta z_{ij} = z_{UAV,ij} - z_{\mathrm{LiDAR},ij} \quad (4)$$

HESSD
12, 5629–5670, 2015

where Δz_{ij} is the elevation difference between the two DEMs in the cell *ij*, UAV_{ij} represents the elevation value of the cell *ij* of the UAV DEM and $Swisstopo_{ij}$ represents the elevation value of the cell *ij* of the LiDAR DEM. Figure 5 shows that absolute elevation differences show virtually no bias (slight positive bias) (mean: −0.199 m). It can also be seen that the LiDAR DEM elevation values are in general higher than those of the UAV DEM; this is clearly visible through the blueish colours along the water stream in ① of Fig. 5a. This is in agreement with the results obtained in the visual comparison of the DEMs (see Sect. 4.2.1).

It is however noteworthy that the majority of the elevation differences in the *Buildings* areas are small (± 0.10 m). From this, one may say that the majority of the elevation differences between the two DEMs are due to existing vegetation and non-static features, such as vehicles on the roads, which are present in one DEM but not in the other.

From Fig. 6 one can see that the data set with less spread is the *Buildings* one – this may be explained by the absence of trees on the top of buildings; the number of outliers for the *All areas* data set is significant and relatively higher when compared to the other two data sets. The variation on the *Roads* data set may be explained by the presence of cars and in some cases by tree canopies that cover part of the road. A summary of the elevation differences statistics is presented in Table 3.

The elevations of the two DEMs were also compared on a selected road area (see dashed polygon in Fig. 5a). This area was defined based on the visual analysis of the aerial orthophoto used to generate the UAV DEM; the LiDAR DEM has only stable and visible landscape elements represented. This area covers approximately 1500 m^2 and his free from cars, trees and man-made elements such as constructions. As can be seen from Fig. 6 and Table 3, the differences between the two DEMs in this area are almost negligible.

HESSD
12, 5629–5670, 2015

4.2.3 Slope and aspect comparison

As can be seen in Fig. 7a, the value of the slope of the two DEMs is similar when there are no trees or vegetation, such as on the top of the buildings. Contrary, the major slope differences occur around buildings where vegetation like bushes and trees exist.

Table 4 presents the descriptive statistics of the slope for the two DEMs and considering two specific land-uses, roads and buildings, plus a mix of all land uses in the case study area. The differentiation of land-uses was obtained using cadastre data. As can be seen, the descriptive statistic values of the two DEMs are not significantly different. The major difference occurs with the maximum slope for all areas and roads; in this case the maximum slope values are significantly different between the two DEMs, and may be due to the presence of trees in the LiDAR DEM that are not represented in the UAV DEM due to the tree-leaves-off condition during the UAV flight.

As can be seen in Fig. 8, the terrain aspect distribution of the two DEMs is very similar.

4.2.4 Delineation of flow paths

Flow paths were delineated using the conventional D8 flow direction algorithm (Jenson and Domingue, 1988) for the three UAV DEMs at different resolutions (0.5, 1.0 and 2.0 m pixel^{-1}) as well as for the LiDAR DEM. The results are presented in Fig. 8 and show that the flow paths delineated using the UAV DEMs followed a realistic path along the side of the road. This behaviour was retained even when the UAV DEM was downsampled to 2 m pixel^{-1} (Fig. 9c); this is in close agreement with the results presented by Sampson et al. (2012), who downsampled terrestrial LiDAR for use in urban inundation models. In comparison to the LiDAR DEM, it is clearly seen that the UAV DEMs can add additional detail to overland flow modelling applications; flow paths obtained using the LiDAR DEM are slightly different from the ones obtained using the UAV-based DEM.

HESSD
12, 5629–5670, 2015

4.3 Discussion

The impact of the flight parameters considered in this study on the DEM quality metrics was not substantial. For example, the quantitative metrics could not have been related to the flight parameters considered in this study. Other flight parameters than the ones considered in this study may have contributed to these results; these factors could be external, such as wind conditions or internal, such as the camera quality and operation mode. This needs further investigation/a different experimental design and goes beyond the scope of this study.

The comparison of the UAV DEM with a LiDAR DEM showed that the two are comparable; the original high resolution of the UAV DEM may contribute to obtain more realistic overland flow patterns even when the DEM resolution is downsampled. UAV imagery can be more frequently updated than conventional DEM production imagery, which is also an important advantage of UAV DEMs.

The range of applications of UAVs in the civil context is already vast, e.g., archaeology (Sauerbier and Eisenbeiss, 2010), precision agriculture (Zhang and Kovacs, 2012) and crowd monitoring (Duives et al., 2014). UAVs have however a strong negative connotation which has motivated both civilian and military sectors to propose alternative names, such as Remotely Piloted Aircraft (RPA) or Unmanned Vehicle System (UVS) (Bennett-Jones, 2014; Eisenbeiss, 2009). While their application in military operations was perhaps their first use, the industry of civil UAVs has been increasing steadily, as illustrated by the number of civil UAVs that has more than doubled since 2008 (Colomina and Molina, 2014). Applications of UAVs are also getting significant visibility in the media, mostly due to privacy (J.-B. Vilmer, personal communication, 2015; Wildi, 2015) and safety issues.

UAVs can take the form of single- or multiple-blade helicopters and fixed-wing aircraft, though other possibilities exist. Eisenbeiss (2009) gives an extensive historical background of the various UAV types. These different UAV forms incorporate different safety features in order to prevent injuries and damages in the event of a flight failure;

HESSD
12, 5629–5670, 2015

these are for example, the incorporation of a parachute. In the case of the eBee UAV, used in this study, its extremely light frame and its gliding capability make it safe in the case of flight failure and hence safe to fly in urban areas. This safety issue is of course a serious concern of the public and of the managers of public space. To respond to this concern, different countries have legislation already in place or being prepared to regulate the public use of UAVs in urban areas and mass gathering events. Nevertheless, we consider that the use of UAVs for civil applications will continue to increase, following the development and improvement of the Unmanned Aerial Systems technology, such as UAV, UAV control and navigation software and sensor technology. As an example of possible new civil applications of UAV imagery, we are currently investigating the potential of UAV imagery for automatic location of sewer inlets and manholes of urban drainage systems, based on image analysis methods.

5 Conclusions

Although detailed and accurate representation of terrain is of paramount importance for flood modelling and assessment, it is challenging for DEMs acquired with traditional methods such as LiDAR or aerial surveys. In this study, we demonstrate the applicability and the advantages of using UAVs to generate very-high-resolution DEMs to be used in urban overland flow and flood modelling. To address this objective, we assessed (i) the influence of flight parameters in the quality of the DEMs produced using UAVs technology, and (ii) the quality of the UAV-based DEM in comparison to the conventional LiDAR-based DEM available in Switzerland. We concluded that:

- UAV platforms and software are a mature technology that deliver satisfactory results for urban overland flow modelling.
- Interestingly, only few dependencies between the flight parameters and DEM quality could be identified. This might be due to variability introduced by other external and internal factors not investigated in detail in this study. Although, at

HESSD
12, 5629–5670, 2015

first sight, this might leave only little potential for optimal experimental design, at second sight this also means that the technology is rather robust against flight altitude, camera pitch settings, image overlapping parameters and thus suitable for practitioners.

– As expected, the most influential flight parameter was the flight altitude, where *lower flights* produce better DEMs. Other flight parameter, such as the effect of sun (e.g., weather conditions), showed some effect on the DEM quality but its effect was clearly weaker than the flight altitude – *overcast weather conditions* are better. Other relationships could not be observed as hypothesized, e.g., camera pitch and image overlapping. For a given flight parameter, the number of samples (flights) may have been a limiting factor to observe trends. In future studies, it would be recommended to conduct additional flight campaigns. By repeating flights with the same parameters in order to quantify how much DEM quality may vary, independently of flight parameters one may also evaluate uncertainty in the elevation data generated.

– Comparing the UAV DEM to a commonly available LiDAR-based DEM, we found that the quality of both DEMs is comparable. The differences between the two DEMs are not substantial, especially when the comparison was conducted in a flat road area without cars, buildings, trees or vegetation. In general, the observed differences are probably mainly explained by the presence of tree leaves in the LiDAR DEM and their absence in the UAV DEM. This is due to fact that the time of the year when the UAV flights were conducted: late winter in tree-leaves-off conditions. When comparing flow paths delineated using the different DEMs, it could be seen that the flow paths obtained using a DEM downsampled (2 m pixel size) from the finer resolution UAV DEM (0.05 m pixel size) retained the major flow path patterns. The flow paths obtained using the liDAR DEM were slightly different from those obtained using the UAV DEMs; this is mostly due to the presence of vegetation and trees in the first DEM. The UAV DEM has two main/practical ad-

HESSD
12, 5629–5670, 2015

vantages over the LiDAR DEM, despite the similarities mentioned above. First, it is more flexible to acquire elevation data using UAVs, especially for small to medium size areas (or catchments), and the second is that if the UAV flights are conducted during winter with tree-leaves-off conditions, DEMs with no tree canopies represented can be produced, which are especially beneficial for land use classification and overland flow processes. Our findings suggest that UAVs can greatly improve overland flow modelling by increasing the detail of terrain representation and also by their inherent flexibility to update existing elevation datasets. The very high resolution possible to obtain using UAV DEMs is also an advantage for urban overland flow and flood modelling purposes. Further research should be carried out towards the development of an urban drainage modelling application in order to assess the real benefit of using very-high resolution DEMs and hydraulic models.

Appendix: Unmanned aerial system

The mini-UAV platform used in the study is a fully autonomous fixed-wing aircraft developed by senseFly SA[7] The UAV is electric-powered, has a wingspan of 0.96 m, and weighs approximately 0.7 kg including a payload of 0.15 kg. The UAV can cover large areas in a reasonable amount of time, which is important for the economic viability of UAV remote sensing. Detailed information is provided in Table A1.

The specifications of the IXUS 127 HS camera part of the Unmanned Aerial System used in this study are presented in Table A2.

Acknowledgements. The authors are grateful for the expert advice received from K. Schindler, ETH Zurich, during the development of this study, especially regarding photogrammetry.

[7] http://www.sensefly.com

HESSD
12, 5629–5670, 2015

References

Allitt, R., Blanksby, J., Djordjevic, S., Maksimovic, C., and Stewart, D.: Investigations into 1-D–1-D and 1-D–2-D urban flood modelling, in: WaPuG Autumn conference, Blackpool, 8, UK, 11–13 November, 2009.

Apel, H., Aronica, G. T., Kreibich, H., and Thieken, A. H.: Flood risk analyses – how detailed do we need to be?, Nat. Hazards, 49, 79–98, doi:10.1007/s11069-008-9277-8, 2009.

Baltsavias, E.: A comparison between photogrammetry and laser scanning, ISPRS Journal of Photogrammetry and Remote Sensing, 54, 83–94, doi:10.1016/S0924-2716(99)00014-3, 1999.

Bennett-Jones, O.: Drones or UAVs? search for a more positive name, BBC news, available at: http://www.bbc.com/news/magazine-25979068 (last access: 30 April 2015), 2014.

Burrough, P. A. and McDonnell, R. A.: Principles of Geographical Information Systems, Oxford University Press, New York, 1988.

Chen, A. S., Djordjević, S., Leandro, J., and Savić, D.: The urban inundation model with bidirectional flow interaction between 2-D overland surface and 1-D sewer networks, in: Novatech, Lyon, France, 465–472, 2007.

Colomina, I. and Molina, P.: Unmanned aerial systems for photogrammetry and remote sensing: a review, ISPRS Journal of Photogrammetry and Remote Sensing, 92, 79–97, doi:10.1016/j.isprsjprs.2014.02.013, 2014.

De Jong, S. M., Hornstra, T., and Maas, H.: An integrated spatial and spectral approach to the classification of Mediterranean land cover types: the SSC method, Int. J. Appl. Earth Obs., 3, 176–183, 2001.

Duives, D. C., Daamen, W., and Hoogendoorn, S.: Trajectory analysis of pedestrian crowd movements at a dutch music festival, in: Pedestrian and Evacuation Dynamics 2012, edited by: Weidmann, U., Kirsch, U., and Schreckenberg, M., Springer International Publishing, Cham, Switzerland, 151–166, available at: http://link.springer.com/chapter/10.1007/978-3-319-02447-9_11 (last access: 30 April 2015), 2014.

Eisenbeiss, H.: UAV Photogrammetry, ETH Zürich Inst. f. Geodäsie u. Photogrammetrie, Zürich, 2009.

Fewtrell, T. J., Duncan, A., Sampson, C. C., Neal, J. C., and Bates, P. D.: Benchmarking urban flood models of varying complexity and scale using high resolution terrestrial lidar data, Phys. Chem. Earth Pt. A/B/C, 36, 281–291, doi:10.1016/j.pce.2010.12.011, 2011.

HESSD
12, 5629–5670, 2015

Hunter, N. M., Bates, P. D., Neelz, S., Pender, G., Villanueva, I., Wright, N. G., Liang, D., Falconer, R. A., Lin, B., Waller, S., Crossley, A. J., and Mason, D. C.: Benchmarking 2-D hydraulic models for urban flooding, in: Proceedings of the ICE – Water Management, 161, 13–30, doi:10.1680/wama.2008.161.1.13, ICE Publishing, London, UK, 2008.

Hutchinson, M. F. and Gallant, J. C.: Digital elevation models and representation of terrain shape, in: Terrain Analysis: Principles and Applications, edited by: Wilson, J. P. and Gallant, J. C., John Wiley and Sons, Inc., New York, USA, 29–50, 2000.

Jenson, S. K. and J. O. Domingue: Extracting topographic structure from digital elevation data for geographic information system analysis, Photogramm. Eng. Rem. S., 54, 1593–1600, 1988.

Kraus, K.: Band 1 Photogrammetrie, Geometrische Informationen aus Photographien und Laserscanneraufnahmen, Walter de Gruyter, Berlin, Germany, ISBN: 3-11-017708-0, 2004.

Küng, O., Strecha, C., Beyeler, A., Zufferey, J.-C., Floreano, D., Fua, P., and Gervaix, F.: The accuracy of automatic photogrammetric techniques on ultra-light UAV imagery, in: UAV-g 2011 – Unmanned Aerial Vehicle in Geomatics, Zurich, Switzerland, available at: http://infoscience.epfl.ch/record/168806 (last access: 30 April 2015), 2011.

Leandro, J., Djordjevic, S., Chen, A., and Savic, D. A.: Flood inundation maps using an improved 1-D/1-D model, in 8th UDM: International Conference on Urban Drainage Modelling, 7–12 September, Tokyo, Japan, available at: http://www.researchgate.net/profile/Dragan_Savic3/publication/257200050_Flood_inundation_maps_using_an_improved_1D1D_model/links/00b7d526185200520f000000.pdf (last access: 30 April 2015), 2009.

Leberl, F., Irschara, A., Pock, T., Meixner, P., Gruber, M., Scholl, S., and Wiechert, A.: Point clouds: LIDAR vs. 3-D vision, Photogramm. Eng. Rem. S., 76, 1123–1134, 2010.

Leitão, J. P., Boonya-aroonnet, S., Prodanovic, D., and Maksimovic, C.: The influence of digital elevation model resolution on overland flow networks for modelling urban pluvial flooding, Water Sci. Technol., 60, 3137–3149, doi:10.2166/wst.2009.754, 2009.

Maksimović, Č., Prodanović, D., Boonya-aroonnet, S., Leitão, J. P., Djordjević, S., and Allitt, R.: Overland flow and pathway analysis for modelling of urban pluvial flooding, J. Hydraul. Res., 47, 512–523, doi:10.1080/00221686.2009.9522027, 2009.

Montgomery, D. C., Peck, E. A., and Vining, G. G.: Introduction to Linear Regression Analysis, Wiley, Hoboken, NJ, ISBN: 978-0-470-54281-1, 2012.

Moy de Vitry, M.: Improving urban flood management with autonomous mini-UAVs, MSc thesis, ETH Zurich, Zurich, Switzerland, 2014.

HESSD
12, 5629–5670, 2015

Pix4-D Support Team: Pix4-D Knowledge Base, Pix4-D Support, available at: https://support.pix4d.com/entries/26825498, last access: 27 April 2015, available at: WebCite at http://www.webcitation.org/6Y6TNZI2U (30 April 2015), 2014.

Podobnikar, T.: Methods for visual quality assessment of a digital terrain model, S. A. P. I. EN. S. Surveys and Perspectives Integrating Environment and Society, 2.2 (May), available at: http://sapiens.revues.org/738 (30 April 2015), 2009.

Reinartz, P., d'Angelo, P., Krauß, T., Poli, D., Jacobsen, K., and Buyuksalih, G.: Benchmarking and quality analysis of Dem generated from high and very high resolution optical stereo satellite data, in: Proceedings of the The 2010 Canadian Geomatics Conference and Symposium of Commission I, ISPRS Convergence in Geomatics – Shaping Canada's Competitive Landscape, Calgary, Alberta, Canada, available at: http://www.isprs.org/proceedings/XXXVIII/part1/09/09_03_Paper_33.pdf (30 April 2015), 2010.

Remondino, F., Barazzetti, L., Nex, F., Scaioni, M., and Sarazzi, D.: UAV Photogrammetry for Mapping and 3d Modeling – current Status and Future Perspectives, International Archives of the Photogrammetry, Remote Sensing and Spatial Information Sciences, 38, Zurich, Switzerland, International Society of Photogrammetry and Remote Sensing (ISPRS), 25–31, 2011.

Sampson, C. C., Fewtrell, T. J., Duncan, A., Shaad, K., Horritt, M. S., and Bates, P. D.: Use of Terrestrial Laser Scanning Data to Drive Decimetric Resolution Urban Inundation Models, Adv. Water Resour., 41, 1–17, doi:10.1016/j.advwatres.2012.02.010, 2012.

Sauerbier, M. and Eisenbeiss, H.: UAVs for the Documentation of Archaeological Excavations, International Archives of Photogrammetry, Remote Sensing and Spatial Information Sciences, 38, Newcastle upon Tyne, UK, 526–531, 2010.

Sona, G., Pinto, L., Pagliari, D., Passoni, D., and Gini, R.: Experimental analysis of different software packages for orientation and digital surface modeling from UAV images, Earth Science Informatics, 7, 97–107, doi:10.1007/s12145-013-0142-2, 2014.

Swisstopo: SWISSIMAGE – Das Digitale Farborthophotomosaik der Schweiz, Eidgenössisches Departement für Verteidigung, Bevölkerungsschutz und Sport VBS, Wabern, Switzerland, 2013.

Triggs, B., McLauchlan, P. F., Hartley, R. I., and Fitzgibbon, A. W.: Bundle adjustment – a modern synthesis, in: Vision Algorithms: Theory and Practice, Lecture Notes in Computer Science, Vol. 1883, edited by: Triggs, B., Zisserman, A., and Szeliski, 298–372, [ISBN: 3-540-67973-1], R., Springer, Berlin, Germany, 2000.

HESSD
12, 5629–5670, 2015

VBS: Technische Verordnung des VBS über die Amtliche Vermessung, available at: http://www.admin.ch/opc/de/classified-compilation/19940126/200807010000/211.432.21.pdf (last access: 23 April 2015), 2008, (in German).

Venables, W. N. and Ripley, B. D.: Modern Applied Statistics with S, Springer, New York, ISBN: 978-0-387-95457-8, 2002.

Vojinovic, Z. and Tutulic, D.: On the use of 1-D and coupled 1-D–2-D modelling approaches for assessment of flood damages in urban areas, Urban Water J., 6, 183–199, 2009.

Wildi, J.: Drones: industry and business applications, in: Drones: From Technology to Policy, Security to Ethics Forum, 30 January, ETH Zurich, Switzerland, 693–712, 2015.

Zhang, C. and Kovacs, J. M.: The application of small unmanned aerial systems for precision agriculture: a review, Precis. Agric., 13, 693–712, doi:10.1007/s11119-012-9274-5, 2012.

HESSD
12, 5629–5670, 2015

Table 1. Qualitative metric classes.

Class	Representation of voids	Representation of buildings edges	Representation of walls	Presence of trees
3	100 % open	Sharp edges	Perfectly represented wall	Not visible
2	50 % open	Little noisy	A straight object	Freckles
1	25 % open	A lot noisy	Unclear	Almost complete
0	0 % open	Chaotic	Nothing	Complete

HESSD
12, 5629–5670, 2015

Table 2. Characteristics of the 16 flights.

Flights	Flight altitude (m)	GSD (cm)	Camera Pitch (°)	Frontal overlap (%)	Lateral overlap (%)	Weather conditions[b]
1	145	4.5	0	80	70	Clear
2	145	4.5	0	70	80	Clear
3	145	4.5	7	70	80	Clear
4[a]	145	4.5	15	70	80	Clear
5	205	6.5	0	70	80	Clear
6	205	6.5	7	70	80	Clear
7	205	6.5	15	70	80	Clear
8	85	2.5	0	70	80	Overcast
9	310	10	0	70	80	Partly cloudy
10	220	7	5	70	80	Clear
11	220	7	5	85	80	Partly cloudy
12	220	7	5	55	80	Clear
13	220	7	5	70	65	Clear
14	220	7	5	70	90	Clear
15	220	7	5	70	70	Clear
16	220	7	5	60	80	Partly cloudy

[a] DEM generated from flight 4 was used for the comparison with the LiDAR DEM.
[b] http://www.erh.noaa.gov/er/box/glossary.htm.

HESSD
12, 5629–5670, 2015

Table 3. Summary statistics of elevation differences.

	Elevation differences (m)			
	All areas	Buildings	Roads	Selected road
Minimum	−12.880	−5.698	−22.880	−0.468
Mean	0.259	0.031	−0.212	0.06
SD	2.037	1.144	2.164	0.119
Maximum	11.930	11.930	6.290	0.306
Number of comparison cells	8.700	1.099	974	375

HESSD
12, 5629–5670, 2015

Table 4. DEMs' slope descriptive statistics (%).

	All areas		Roads		Buildings	
	UAV	LiDAR	UAV	LiDAR	UAV	LiDAR
Minimum	0.017	0.051	0.107	0	0.077	0.088
Maximum	430.592	595.917	153.929	595.917	214.135	310.699
Mean	38.036	21.908	10.916	21.620	29.206	36.540
SD	48.394	20.560	11.521	60.791	34.684	42.121

HESSD
12, 5629–5670, 2015

Table A1. Detailed characteristics of the UAV.

Wingspan	0.96 m
Wing area	0.25 m
Typical Weight	0.7 kg
Payload	16 MP camera, electronically integrated and controlled
Battery	3-cell Lithium-Polymer
Capacity	1800 mAh
Endurance	45 min of flight time
Propulsion	Electric brushless motor
Nominal cruise speed	36–72 $km\,h^{-1}$ (10–20 $m\,s^{-1}$)
Wind resistance	up to 45 $km\,h^{-1}$ (12 $m\,s^{-1}$)
Mapping area	coverage up to 10 km^2
Remote control	2.4 GHZ, range: approx. 1 km, certification: CE. FCC
Data communication	2.4 GHZ, range: approx. 3 km, certification: FCC Part 15.247
Navigation	Autonomous flight and landing, up to 50 waypoints direction
Material	Styrofoam
Cost (in 2015)	Approx. CHF 20 000 (UAV + camera + software)

HESSD
12, 5629–5670, 2015

Table A2. Specifications of the Canon IXUS 127 HS.

Camera effective pixels	Approx. 16.1 million pixels
Lens focal length	5× zoom: 4.3 (W) – 21.5 (T) mm (35 mm film equivalent: 24 (W) – 120 (T) mm)
File formats	Exif 2.3 (JPEG)
Dimensions	93.2 × 57.0 × 20.0 mm (Based on CIPA Guidelines)
Weight	Approx. 0.135 kg (including batteries and memory card)

HESSD
12, 5629–5670, 2015

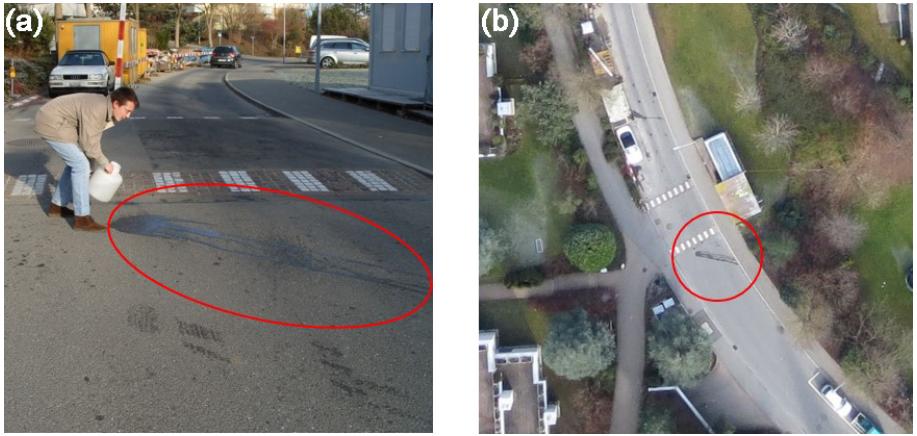

Figure 1. Example of the field experiments conducted to calculate the terrain flow direction and flow path delineation metrics. **(a)** Terrain aspect and Flow path field experiment preparation, **(b)** aerial photo of field experiment location.

HESSD
12, 5629–5670, 2015

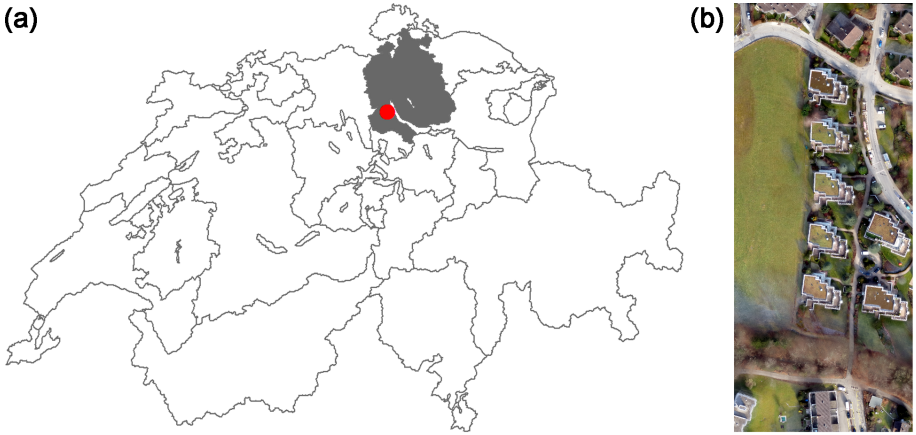

Figure 2. Case study location and area aerial photo. **(a)** Adliswil (Zurich Canton, Switzerland). **(b)** Case study areal aerial photo (130 × 300 m).

HESSD
12, 5629–5670, 2015

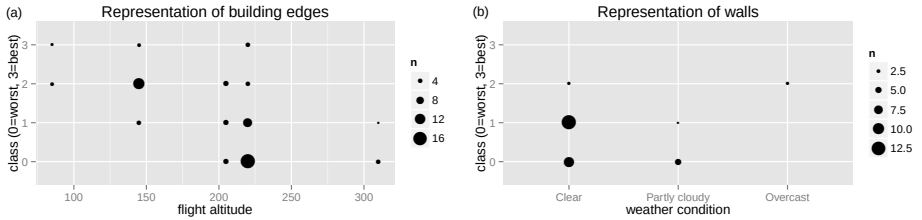

Figure 3. Relationship between the quality of the representation of building edges and flight altitude. The size of the dots is proportional to the number of observed metrics with identical quality class and altitude or weather condition, respectively. **(a)** Representation of building edges. **(b)** Representation of walls.

HESSD
12, 5629–5670, 2015

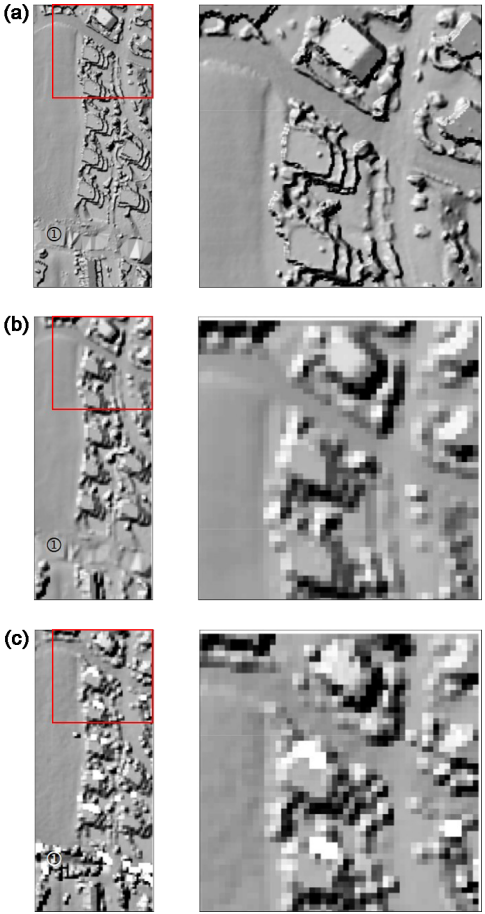

Figure 4. Visual comparison of the UAV DEM and LiDAR DEM. **(a)** UAV DEM (downsampled to 0.5 m pixel^{-1}). **(b)** UAV DEM (downsampled to 2 m pixel^{-1}). **(c)** LiDAR DEM (2 m pixel^{-1}).

HESSD
12, 5629–5670, 2015

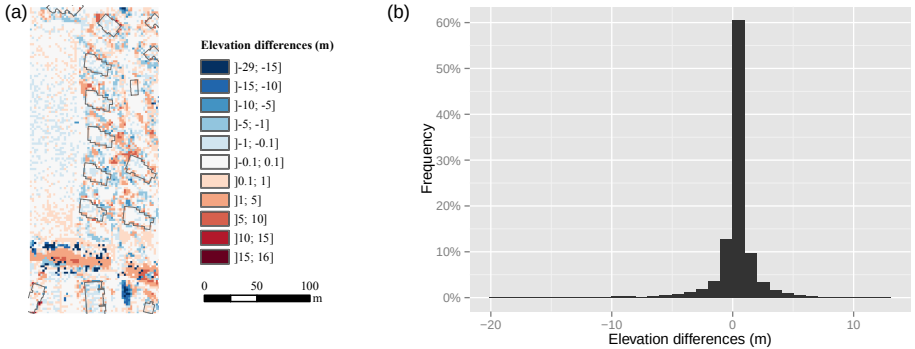

Figure 5. Elevation differences between the UAV DEM and the LiDAR DEM (both with 2 m pixel^{-1} resolution). The dashed line polygon represents a road area selected based on visual analysis of the UAV orthophoto and used to compare the elevation of the two DEMs without objects such as trees, cars or other man-made elements; light grey polygons represent buildings. **(a)** Spatial distribution. **(b)** Histogram.

HESSD
12, 5629–5670, 2015

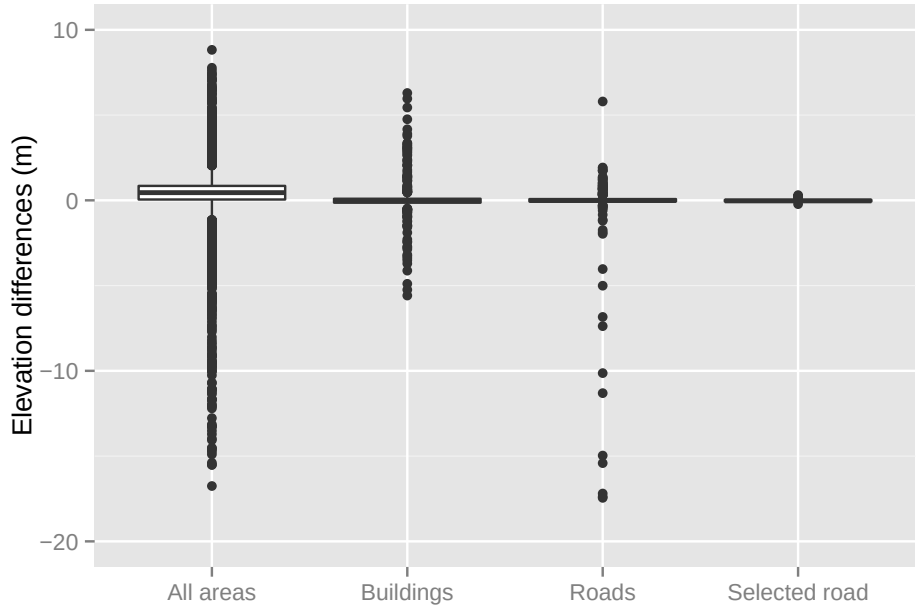

Figure 6. Elevation differences between the UAV DEM and the LiDAR DEM for three types of areas (width of box plot represents the amount of data points used to generate the box-plot).

HESSD
12, 5629–5670, 2015

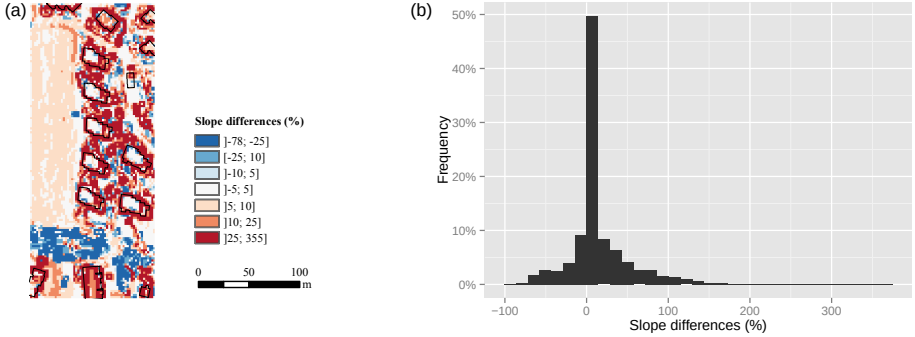

Figure 7. Slope differences between the UAV DEM and the LiDAR DEM. **(a)** Spatial distribution. **(b)** Histogram.

HESSD
12, 5629–5670, 2015

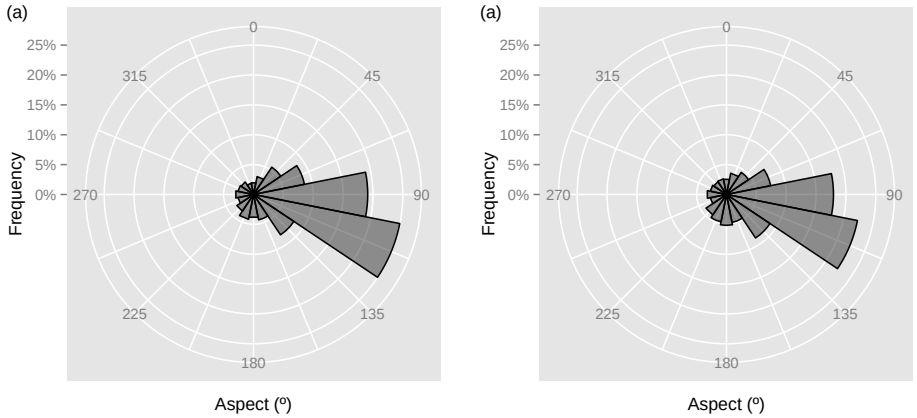

Figure 8. Distribution of terrain aspect. The aspect values are in degrees. The outer number represent the cardinal directions in degrees. **(a)** UAV DEM. **(b)** LiDAR DEM.

HESSD
12, 5629–5670, 2015

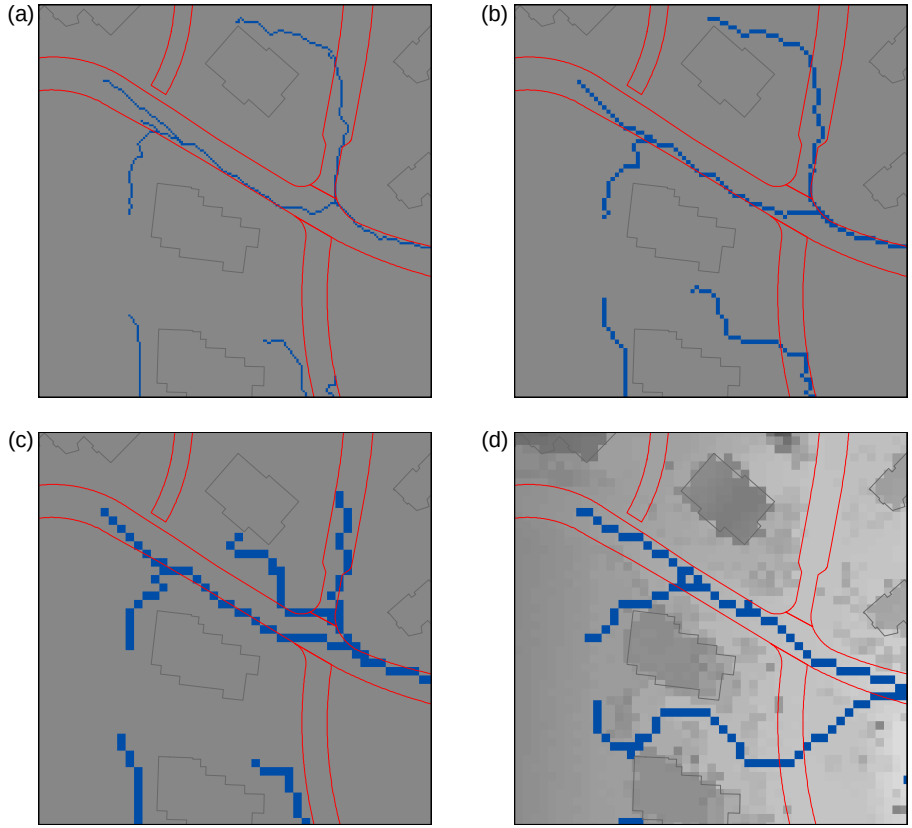

Figure 9. DEM-based flow path delineation. **(a)** UAV DEM (0.5 m pixel^{-1}). **(b)** UAV DEM (1 m pixel^{-1}). **(c)** UAV DEM (downsampled to 2 m pixel^{-1}). **(d)** LiDAR DEM (2 m pixel^{-1}).

HESSD
12, 5629–5670, 2015